MOOSE Project Part 1

Anthony Cowan
NCSU - NE533

Contents

---

1 Introduction

The modeling and simulation of nuclear fuel performance are critical to ensuring the safety and efficiency of nuclear reactors. This project focuses on the steady-state and transient thermal behavior of a fuel pellet system using the MOOSE (Multiphysics Object-Oriented Simulation Environment) framework. The objective is to compute the temperature distribution within a cylindrical fuel pellet under different thermal conditions and compare the results against an analytical solution.

The required models are 1) a steady-state, constant thermal conductivity system, 2) a time-dependent, constant thermal conductivity system, and 3) a temperature-dependent thermal conductivity application to the previous two systems. The first requires a temperature profile to be reported, and the second demands a transient centerline temperature.

The following report documents the approach and analysis of the stipulated problem statement, including the methods, results, and discussion of each aspect.

2 Methods

To obtain a final solution to the problem set, several steps were taken, including 1) the construction of a simple steady-state model, 2) a mesh convergence study for the steady-state model, 3) adding transient capabilities to the steady-state model, and 4) augmenting the thermal conductivity of all materials, in both the steady-state and transient cases, to rely on temperature-dependent empirical models.

2.1 Steady-State Model

The first step to establishing the steady-state model was defining geometric and material parameters. For the former, all parameters were taken from the problem definition. UO_2 fuel, helium gap, and zirconium cladding were selected to locate material properties. These parameters were found through differing sources; all thermophysical properties were found in the "Lecture 3" slide deck on slide 31 for the fuel and cladding. For the gap, it was assumed that it was a pure helium system; properties were found in an article that detailed a helium-related study [2]. Table 1 outlines geometric parameters, and Table 2 details the located thermophysical properties. All material properties were put into the "Materials" block using "ADHeatConductionMaterial" and "ADGenericConstantMaterial".

Table 1: Geometric Parameters

Block	$\mathbf{r_{min}}$ **(cm)**	$\mathbf{r_{max}}$ **(cm)**	**z (cm)**
Fuel	0	0.5	1
Gap	0.5	0.505	1
Clad	0.505	0.605	1

Table 2: Thermophysical Properties

Properties	$\mathbf{UO_2}$	**He**	**Zr**
k_{th} (W/cm-K)	0.03	0.15×10^{-2}	0.17
c (J/g-K)	0.33	5.19	0.35
ρ (g/cm^3)	10.98	0.18×10^{-3}	6.50

The governing equation that is used to solve this problem is the heat conduction equation; the three-dimensional, transient form of the equation is defined as

$$\rho(t,\vec{x})c(t,\vec{x})\frac{\partial T}{\partial t} = \nabla k(t,\vec{x})\nabla T(t,\vec{x}) + \dot{q} \tag{1}$$

Equation (1) can be simplified by applying some reasonable assumptions, the first being that the problem is spatially 2D (RZ). After this, Equation (1) becomes

$$\rho(t,r,z)c(t,r,z)\frac{\partial T}{\partial t} = \nabla k(t,r,z)\nabla T(t,r,z) + \dot{q} \tag{2}$$

The next assumption is that the system is steady-state or $\frac{\partial T}{\partial t} = 0$; Equation (2) becomes

$$0 = \nabla k(r,z)\nabla T(r,z) + \dot{q} \tag{3}$$

Finally, it is assumed that the thermal conductivity is a constant; this produces the following equation:

$$0 = k\nabla^2 T + \dot{q} \tag{4}$$

This second-order partial differential equation (PDE) requires at least two boundary conditions to be solved. The first is a Dirichlet boundary condition established by the problem statement, and the second is a zero-flux, reflective Neumann boundary condition at the centerline of the fuel pellet, imposing that only half of the geometry needs to be modeled. A zero-flux, reflective Neumann boundary condition was added to the top and bottom boundaries to produce a 1D calculation per the problem requirements. Our final equation definition now becomes

$$0 = k\nabla^2 T(r,z) + \dot{q}$$

$$\nabla T(r,0) = \nabla T(r,1) = \nabla T(0,z) = 0, T(0.605,z) = 550 \tag{5}$$

The governing equation was implemented in MOOSE's "Kernels" block; the first term was added using the Heat Transfer Module types of "ADHeatConduction" and the second term with "HeatSource". The given linear heat rate (350 W/cm) had to be changed to a volumetric heat rate, taking its quotient with the surface area of the top face of the fuel; this calculation was placed in the "Functions" block as a "ParsedFunction", as shown in Equation (6).

$$VHR = \frac{LHR}{\pi R_f^2} \tag{6}$$

The boundary conditions were established in the "BCs" block using "ADDirichletBC" and "ADNeumannBC." The "Variables" block specified the variable "T" to inform MOOSE it should solve for that variable. The problem was designated as steady-state by specifying "type = Steady" in the "Executioner" block.

The temperature profile was probed by establishing a "VectorPostprocessor" using "LineValueSampler", which samples the variable, T, along a vector with a prescribed start and end point; this was chosen to span the entire radius of the fuel pellet at z=0.5 cm with 1000 sampling points.

All tolerances, solver, and preconditioning settings were selected through trial and error to produce a reasonable solution.

2.2 Mesh Convergence

The "Mesh" block is the final piece required to complete the MOOSE input file. A single square mesh was created for simplicity, ranging from $0 \leq r \leq 0.605$ cm and $0 \leq z \leq 1$ cm. The coordinate system was set to "RZ" to keep calculations and boundary condition definitions consistent. The elements in the mesh were then assigned subdomain IDs associated with each material, as defined by their radius ranges, which are shown in Table 1, using "SubdomainBoundingBoxGenerator".

A mesh convergence study was conducted to find a suitable mesh refinement for a reasonable solution. To quantify convergence, both a qualitative and an error assessment were performed, where the error is computed using the L2 norm, which is defined as

$$||T||_2 = \sqrt{(T^h - T)^2} \tag{7}$$

where T^h is the numerical solution generated by MOOSE and T is the analytic solution for the steady-state, constant k_{th} system, which is represented by

$$T_f(r) = T_g(0.5) + \frac{VHR(R_f^2 - r^2)}{4k_f} \tag{8}$$

$$T_g(r) = T_c(0.505) - \ln\left(\frac{r}{R_g}\right)\frac{LHR}{2\pi k_g} \tag{9}$$

$$T_c(r) = T_{oc} - \ln\left(\frac{r}{R_c}\right)\frac{LHR}{2\pi k_c} \tag{10}$$

$$T(r) = \begin{cases} T_f(r), & 0 \leq r \leq R_f \\ T_g(r), & R_f < r \leq R_g \\ T_c(r), & R_g < r \leq R_c \end{cases} \tag{11}$$

where T_f, T_g, and T_c are the analytical temperature profile solutions for the fuel, gap, and cladding, respectively; T_{oc} is the temperature established by the Dirichlet boundary condition; and VHR and LHR are the volumetric heat rate and linear heat rates. Note that this subscript notation remains consistent for any other material or geometric parameters shown in the equations above.

The convergence study began with $n_x = 75$ and $n_y = 1$, where each represents the number of divisions for the elements along their respective axes. The values were then doubled until a reasonable error margin was achieved. The final mesh specifications were also used for the transient and temperature-dependent models.

2.3 Transient Model

For the transient model, an assumption of a constant thermal conductivity was applied to Equation (2); this produces the following equation:

$$\rho(t,r,z)c(t,r,z)\frac{\partial T}{\partial t} = k\nabla^2 T(t,r,z) + \dot{q} \tag{12}$$

A third kernel sub-block, "ADHeatConductionTimeDerivative," was added to account for the time-derivative term. The executioner type was changed to "Transient," and start and end times of 0 and 100 seconds were prescribed. "IterationAdaptiveDT" was also built in to allow for adaptive time-stepping according to an optimal number of non-linear solver iterations; this significantly reduced simulation time.

The final step was changing the LHR to a time-dependent form, shown in Equation (13), as stipulated by the problem.

$$LHR = 350\exp\left(\frac{(t-20)^2}{2}\right) + 350 \text{ W/cm} \tag{13}$$

2.4 Temperature-Dependent Thermal Conductivity

Equations (2) and (3) are revisited to account for temperature-dependent thermal conductivity. Empirical fuel and gap materials models were found in the "Lecture 3" slide deck on slides 15 and 26, respectively. A model for the cladding was found in literature[1]; all of the models are presented below.

$$k_f = \frac{1}{100}\left[\frac{100}{7.5408 + 17.629t + 3.6142t^2} + \frac{6400}{t^{5/2}}\exp\left(\frac{-16.35}{t}\right)\right] \text{ W/cm} - \text{K} \tag{14}$$

$$k_g = 16 \times 10^{-6}\ T^{0.79} \text{ W/cm} - \text{K} \tag{15}$$

$$k_c = \frac{1}{100}\left[8.8527 + 7.0820 \times 10^{-3}\ T + 2.5329 \times 10^{-6}\ T^2 + 2.9918 \times 10^{3}\ T^{-1}\right] \text{ W/cm} - \text{K} \tag{16}$$

where $t = \frac{T}{1000}$. Each of the empirical models was integrated into the MOOSE file by adding them as a "ParsedFunction" in the "Functions" block and calling them using "thermal_ conductivity_temperature_function" in the "ADHeatConductionMaterial" sub-blocks. Everything else remained consistent regarding the steady-state and transient models.

3 Results and Discussion

3.1 Mesh Convergence

As shown in Figure 1a, the solution was computed starting with $n_x = 75$ and $n_y = 1$, and a reasonable solution was reached with $n_x = 600$ and $n_y = 8$. Beyond this value, diminishing returns were evident in the L2 norm, shown in Figure 1b, so these parameters were selected for all models. It is worth noting that the spike in error in the gap region likely stems from the method of creating the mesh; with the equal division, a small fraction of elements were contained within the gap region. A more satisfactory approach could involve separate meshing for each block, allowing for finer tuning of the element population and likely reducing the gap and fuel solution error.

3.2 Steady State

The results from the steady-state simulations, including the constant- and temperature-dependent k_{th} cases, are outlined in Figure 2a. It was established that the constant k_{th} case agrees favorably with the analytical solution.

To dissect the impetus behind the difference in results between the two cases, a plot of the thermal conductivities over the overall temperature range is shown in Figure 3b. A volume-average calculation of the thermal conductivity between the minimum (550K) and relative maximum (2000K) was carried out to determine the overall shift in the system's thermal conductivity as the system reaches equilibrium; the results of this calculation are shown in Figure 2c.

The outcome of this plot presents a fair indication of why the temperature profile generally goes down; the thermal conductivity, on average, increases with temperature, allowing more of the heat to diffuse to the heat sink.

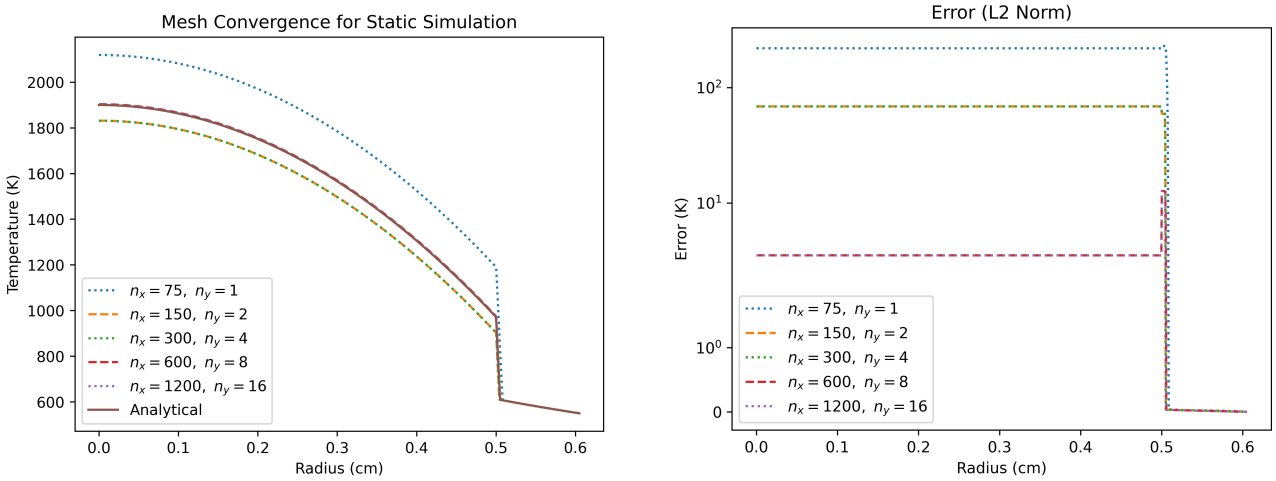

(a) (b)

Figure 1: Mesh Convergence Study Results (a) and Error from L2 norm (b)

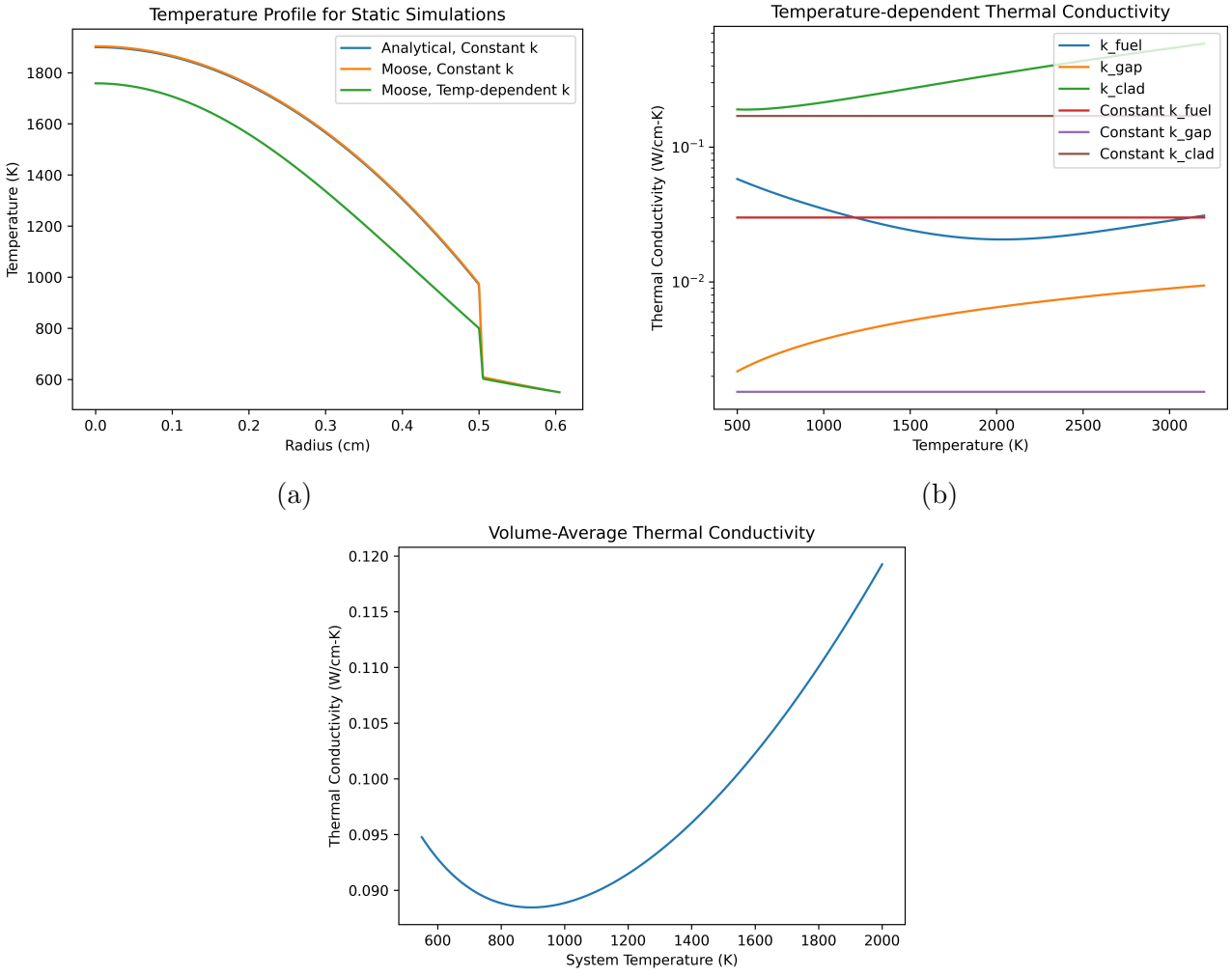

(a) (b)

(c)

Figure 2: Steady-state temperature profiles (a), temperature-dependent k_{th} functions (b), and volume-average thermal conductivity

3.3 Transient

The results from the transient simulations, including the constant- and temperature-dependent k_{th} cases, are outlined in Figure 3a. A plot of the LHR versus time is presented in Figure 3 to provide more context to the highly transient portion of Figure 3a between 20 and 40 seconds. The LHR is identical to the steady-state case after this transient event, so the centerline temperatures are expected to approach those in the steady-state case in this timeframe. This anticipation is confirmed as the centerline temperatures are visually the same between Figures 2a and 3a.

The general decrease in temperature is also observed here, which follows the logic established in the steady-state model as the temperature range is still valid.

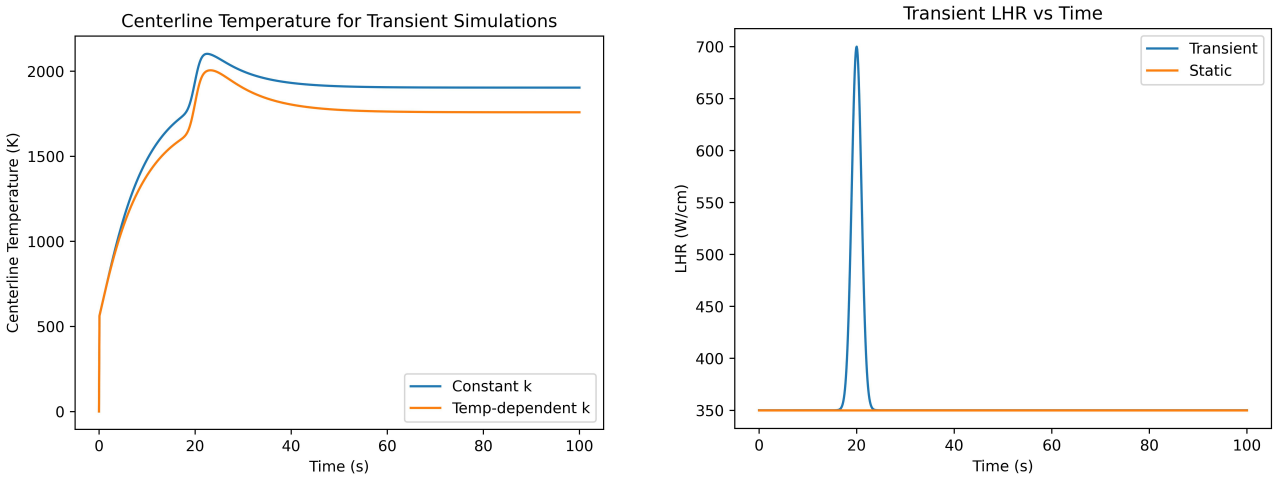

(a) (b)

Figure 3: Transient centerline temperature vs time (a) and LHR temporal evolution (b)

4 Conclusion

This study's results demonstrate the MOOSE framework's effectiveness in modeling the steady-state and transient thermal behavior of a nuclear fuel pellet. A mesh convergence study established that a mesh refinement of n_x=600 and n_y=8 provided a reasonable balance between accuracy and computational efficiency. The steady-state temperature profile for constant thermal conductivity showed good agreement with the analytical solution. The temperature-dependent thermal conductivity model showed a lower temperature overall, which aligned well with the average change in thermal conductivity from low to high temperatures.

Transient simulations confirmed that the temperature evolution follows expected physical trends, with temperatures stabilizing after the transient heat pulse. The decreased centerline temperature for the temperature-dependent conductivity case aligns with the volume-averaged thermal conductivity calculations.

Future work includes adding more control to the mesh of individual blocks and additional complexity to account for other fuel phenomena.

References

[1] JK Fink and L Leibowitz. Thermal conductivity of zirconium. *Journal of Nuclear Materials*, 226(1-2):44–50, 1995.

[2] Jiaping Yang, Cheng Peng Tan, and Eng Hong Ong. Heat transfer enhancement by helium gas filled in a hard disk drive enclosure. In *ASME International Mechanical Engineering Congress and Exposition*, volume 44281, pages 155–159, 2010.